Ionics (2020) 26:4455–4462
https://doi.org/10.1007/s11581-020-03621-6

ORIGINAL PAPER

Enhanced electrochemical performance of Li-rich $Li[Li_{0.2}Mn_{0.52}Ni_{0.13}Co_{0.13}V_{0.02}]O_2$ cathode materials for lithium ion batteries by $Li_{1.13}Mn_{0.47}Ni_{0.2}Co_{0.2}O_2$ coating

Li Zhao[1] · Yingying Sun[1] · Kexin Song[1] · Fei Ding[2]

Received: 19 January 2020 / Revised: 1 May 2020 / Accepted: 12 May 2020 / Published online: 4 June 2020

Abstract

Li-rich layered oxides are the most promising cathode candidate for lithium ion batteries with high specific energy. In this work, $Li_{1.13}Mn_{0.47}Ni_{0.2}Co_{0.2}O_2$-coated Li $[Li_{0.2}Mn_{0.52}Ni_{0.13}Co_{0.13}\ V_{0.02}]O_2$ cathode materials were synthesized via a sol–gel method, and their electrochemical performance was evaluated. Structural and morphological characterizations of the materials demonstrate that $Li[Li_{0.2}Mn_{0.52}Ni_{0.13}Co_{0.13}V_{0.02}]O_2$ particles are covered by $Li_{1.13}Mn_{0.47}Ni_{0.2}Co_{0.2}O_2$ particles. Moreover, the $Li_{1.13}Mn_{0.47}Ni_{0.2}Co_{0.2}O_2$ coating has no obvious effect on the crystal structure of Li-rich materials. The specific capacity, cycle performance, and rate capability of Li-rich materials are significantly improved with the coating of $Li_{1.13}Mn_{0.47}Ni_{0.2}Co_{0.2}O_2$. Materials coated with 1 wt% to 3 wt% $Li_{1.13}Mn_{0.47}Ni_{0.2}Co_{0.2}O_2$ exhibit the highest capacity retention of 93% after 100 cycles at 1 C, which is 10% higher than that of the uncoated one. The specific capacity of 3 wt% $Li_{1.13}Mn_{0.47}Ni_{0.2}Co_{0.2}O_2$-coated material is 115.9 mAh g^{-1} at 5 C, and that of the blank sample is 89.8 mAh g^{-1} under the same condition. The cyclic voltammetry and electrochemical impedance spectra reveal that the enhanced cycle performance and rate capability of the surface-modified Li-rich materials are due to the presence of the $Li_{1.13}Mn_{0.47}Ni_{0.2}Co_{0.2}O_2$ coating layer, which restrains structural transformation with cycling and decreases the charge-transfer resistance of the materials.

Keywords Lithium rich material · Surface coating · Cathode material · Lithium ion batteries

Introduction

Lithium-ion batteries (LIBs) are extensively used in many fields due to their high energy density and operating voltage [1–5]. However, the available energy density of LIBs remains problematic for market requirements, especially for hybrid electric vehicles (HEVs) and electric vehicles (EVs). Numerous materials have been extensively investigated to increase the energy density of LIBs for new applications [6–11]. Li-rich layered oxides, which are denoted as $xLi_2MnO_3\cdot(1-x)LiMO_2$ (M = Ni, Co, Mn, or combinations) or $Li[Li_xM_{1-x}]O_2$ (as a layer type), have attracted considerable attention due to their higher discharge capacity (> 250 mAh g^{-1}) [12–15] compared with that of conventional cathode materials (100–160 mAh g^{-1}). Li-rich layered oxides (such as $Li_{1.2}Mn_{0.54}Ni_{0.13}Co_{0.13}O_2$) have been proven to be one of the most promising cathode materials for next-generation LIBs due to their high discharge capacity, high operating potential (4.6 V to 4.8 V vs. Li^+/Li), low cost, and hypotoxicity. However, with further research, some drawbacks have been detected [16–18]. Li-rich layered oxides suffer from an irreversible capacity due to elimination of Li_2O from the Li_2MnO_3 component when charged to 4.5 V (vs. Li^+/Li) in the first cycle, leading to a low initial coulombic efficiency. This process is accompanied with the removal of oxygen-ion vacancies, thereby reducing the number of Li^+ ion insertion sites in subsequent cycles. The average voltage of Li-rich cathodes gradually decreases when they are cycled above 4.5 V by layered-to-spinel phase transformation, resulting in significant reduction in the energy density of LIBs. Meanwhile, the low electronic conductivity and poor lithium ion diffusion coefficient of the Li_2MnO_3 component leads to poor rate capability.

✉ Li Zhao
dhx907@hit.edu.cn

[1] School of Chemistry and Chemical Engineering, Harbin Institute of Technology, Harbin 150001, People's Republic of China

[2] Science and Technology on Power Sources Laboratory, Tianjin Institute of Power Sources, Tianjin 300384, People's Republic of China

Intensive research has been conducted to improve the electrochemical properties of Li-rich layered oxides by using surface coating [19–21], mild acidic treatment [22, 23], and ionic substitution [23–27]. Surface coating is a feasible approach used to improve the cycling stability and rate capability of Li-rich layered oxides. The coating layer protects the active materials against the attack of hydrofluoric acid by separating them from the electrolyte to suppress the structural transformation of cathode materials at high operating voltages. The coating layer leaves oxygen vacancies during the initial charge for subsequent Li^+ intercalation. Various compounds, such as carbon, metallic phosphates, oxides, and fluorides, have been explored as coating layers. However, most of these materials are non-electrochemically active and lead to decreased cathode gravimetric energy density.

Scholars have proposed a newly designed route [28], wherein coating materials can react with Li^+ and deliver an additional capacity during the charge–discharge process. Li [29] successfully coated layered $Li[Li_{0.2}Mn_{0.52}Ni_{0.13}Co_{0.13}V_{0.02}]O_2$ with FeF_3 through precipitation and performed electrochemical tests; the results showed that the FeF_3-coated $Li[Li_{0.2}Mn_{0.52}Ni_{0.13}Co_{0.13}V_{0.02}]O_2$ cathode shows higher coulombic efficiency, rate capability, and thermal stability as well as longer cycle life than the bare cathode. Hence, the coating material should contain active materials with good cycle performance. The layered Li-rich cathode material $Li_{1.13}[Ni_{0.2}Co_{0.2}Mn_{0.47}]O_2$ has a high capacity retention of 95.9% at 0.5 C after 50 cycles and a reversible capacity of 218.2 mAh g^{-1} at 0.1 C. The material has a lithium ion diffusion coefficient of 2.09×10^{-11} cm^2 s^{-1} and, importantly, a very low charge-transfer resistance Rct. Thus, $Li_{1.13}[Ni_{0.2}Co_{0.2}Mn_{0.47}]O_2$ could be an effective coating material for layered Li-rich cathodes.

In this work, Li-rich layered oxide $Li[Li_{0.2}Mn_{0.52}Ni_{0.13}Co_{0.13}V_{0.02}]O_2$ materials coated with $Li_{1.13}[Ni_{0.2}Co_{0.2}Mn_{0.47}]O_2$ were fabricated via sol–gel method. The influences of coating layer on the microstructure, morphology, and electrochemical performance of the materials were investigated. $Li_{1.13}[Ni_{0.2}Co_{0.2}Mn_{0.47}]O_2$-coated $Li[Li_{0.2}Mn_{0.52}Ni_{0.13}Co_{0.13}V_{0.02}]O_2$ materials exhibit higher specific capacity and better cycle performance than the bare material.

Experimental

Synthesis of cathode materials

The cathode material $Li[Li_{0.2}Mn_{0.52}Ni_{0.13}Co_{0.13}V_{0.02}]O_2$ was synthesized by sol–gel method using glycolic acid as a chelating agent. Stoichiometric amounts of $Mn(CH_3COO)_2 \cdot 4H_2O$, $Ni(CH_3COO)_2 \cdot 4H_2O$, $Co(CH_3COO)_2 \cdot 4H_2O$ $LiCH_3COO \cdot 2H_2O$, and NH_4VO_3 were dissolved in distilled water with 5% $LiCH_3COO \cdot 2H_2O$. The solution was added slowly with 2.0 mol L^{-1} glycolic acid solution under continuous stirring. The mole ratio of glycolic acid to all metal ions was 1:1. The pH of the mixture was adjusted to 7.5 by adding ammonium hydroxide. The solution was evaporated under continuous stirring at 95 °C until a viscid purple aquogel was formed. After drying at 120 °C for 12 h in the vacuum oven, the xerogel was crushed and heated at 450 °C for 5 h. The resulting powder was labeled as A.

Stoichiometric amounts (Li/Mn/Ni/Co = 1.13:0.47:0.2:0.2) of $LiCH_3COO \cdot 2H_2O$, $Mn(CH_3COO)_2 \cdot 4H_2O$, $Ni(CH_3COO)_2 \cdot 4H_2O$, and $Co(CH_3COO)_2 \cdot 4H_2O$ were dissolved in distilled water with 5% $LiCH_3COO \cdot 2H_2O$. The solution was slowly added with 2.0 mol L^{-1} glycolic acid solution under continuous stirring. The mole ratio of glycolic acid to all metal ions was 1:1. The pH of the mixture was adjusted to 7.5 by adding ammonium hydroxide. The resulting solution was labeled as B. The resulting powder A was added into the resulting solution B. After drying at 120 °C for 12 h in the vacuum oven, the mixture was crushed and sintered in the furnace at 900 °C for 12 h to obtain $Li_{1.13}Mn_{0.47}Ni_{0.2}Co_{0.2}O_2$-coated $Li[Li_{0.2}Mn_{0.52}Ni_{0.13}Co_{0.13}V_{0.02}]O_2$.The materials coated with 0 wt%, 1 wt%, 3 wt%, 5 wt%, and 7 wt% $Li_{1.13}Mn_{0.47}Ni_{0.2}Co_{0.2}O_2$ were named M0, M1, M3, M5, and M7, respectively.

Characterization of the prepared materials

The crystal structure of the synthesized materials was examined by powder X-ray diffractometer (XRD, Rigaku RINT2000 with Cu-Kα radiation) within the 2θ range of 10° to 80° with a scan rate of 6° min^{-1}. Particle surface morphology and size of the materials were evaluated using scanning electron microscope (SEM, Hitachi SU8000) at 10.0 kV.

Electrochemical measurements

Electrochemical properties of the synthesized materials were evaluated using coin-type half-cells (CR2032). The coin-type half-cell consists of a positive and a Li metal negative, which were separated by a porous polypropylene film (Celgard2400). $LiPF_6$ (1 mol L^{-1}) was used as electrolyte. For the positive electrode, the synthesized powder was mixed with acetylene black and a PVDF binder in 8:1:1 ratio and dissolved in *N*-methyl-2-pyrrolidone (NMP). The slurry was spread onto a smooth aluminum foil and dried at 100 °C for 12 h in the vacuum oven. The obtained electrode film was squeezed and cut into a circular disk (d = 12 mm). The typical active material loading level was 6.0 ± 0.1 mg cm^{-2}. The coin-type cells were packaged in an argon-filled glove box.

Charge–discharge tests were carried out within the voltage range of 2.0–4.8 V (vs. Li^+/Li) by using Neware instrument. Various current densities, which correspond to 0.1 C to 5.0 C

(1 C = 250 mAh g^{-1}), were applied to evaluate rate capability. Cyclic voltammogram (CV) was obtained using CHI430 electrochemical workstation from 2.0 to 4.8 V with a scanning rate of 0.1 mV s^{-1}. Electrochemical impedance spectroscopy (EIS) was performed using a M2273 electrochemical workstation within the frequency range of 100 KHz to 10 mHz with an amplitude of 10 mV.

Results and discussion

XRD and SEM characterization

Figure 1 presents the X-ray diffraction patterns of the synthesized powder materials. All diffraction peaks of the prepared samples indicate that Li-rich layered oxides are present in the hexagonal α-$NaFeO_2$ structure and belong to a space group of R-3m. The characteristic peaks of the samples are consistent with the standard peak of the layered structure phase of $Li[Li_{0.2}Mn_{0.54}Ni_{0.13}Co_{0.13}]O_2$. No impurities were detected on the samples, confirming that the coated layer had no significant influence on the structure of $Li[Li_{0.2}Mn_{0.52}Ni_{0.13}Co_{0.13}V_{0.02}]O_2$. No diffraction peaks for $Li_{1.13}Mn_{0.47}Ni_{0.2}Co_{0.2}O_2$ were also detected, which may be due to poor crystallinity or low quantity [30]. Additional diffraction peaks between 20° and 25° correspond to the $LiMn_6$ cation arrangement in the transition metal layer of monoclinic Li_2MnO_3 with the C2/m space group. The separations between the adjacent peaks of (006)/(102) and (018)/(110) were clearly observed, implying the formation of the samples with a typical layered structure [31].

Table 1 demonstrates the lattice parameters of $Li_{1.13}Mn_{0.47}Ni_{0.2}Co_{0.2}O_2$-coated $Li[Li_{0.2}Mn_{0.52}Ni_{0.13}Co_{0.13}V_{0.02}]O_2$. The value of c/a corresponds to the stability of the layered structure, and the I(003)/I(104) intensity ratio is an important symbol used to characterize the extent of cation mixing between Ni^{2+} and Li^+ due to their similar ionic radii. All samples show high values of c/a (higher than 4.90) and I(003)/I(104) peak ratio (larger than 1.2), indicating that the prepared materials formed a stable layer structure and low cation mixing degree. The low cation mixing improves the cycling stability in $Li_{1.13}Mn_{0.47}Ni_{0.2}Co_{0.2}O_2$-coated $Li[Li_{0.2}Mn_{0.52}Ni_{0.13}Co_{0.13}V_{0.02}]O_2$ materials [32].

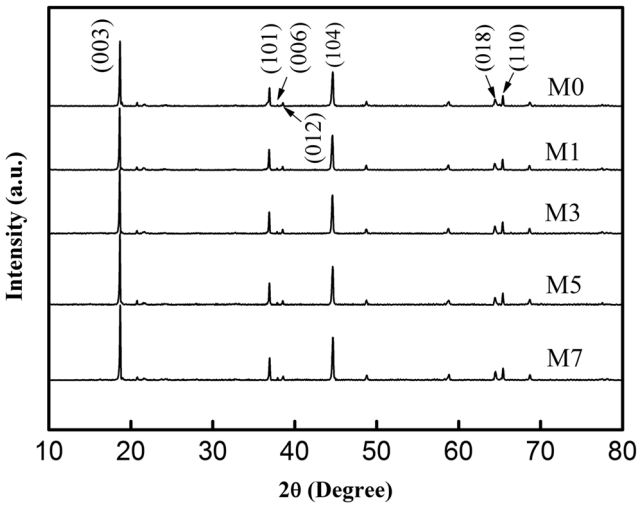

Fig. 1 XRD patterns of samples

Table 1 Lattice parameters of $Li_{1.13}Mn_{0.47}Ni_{0.2}Co_{0.2}O_2$-coated samples

Samples	c/a ratio	$I_{(003)}/I_{(104)}$	$I_{(006)}+I_{(012)})/I_{(101)}$
M0	4.950	1.826	0.246
M1	4.981	1.922	0.219
M3	5.039	1.940	0.211
M5	4.967	1.889	0.269
M7	4.956	1.859	0.282

Powder morphologies were observed by SEM (Fig. 2). The samples are composed of microparticles with sizes of 0.5–2 μm. The crystalline grain size of the coated samples did not change significantly due to the low content of $Li_{1.13}Mn_{0.47}Ni_{0.2}Co_{0.2}O_2$. Small $Li_{1.13}Mn_{0.47}Ni_{0.2}Co_{0.2}O_2$ particles were found on the surface layer (Fig. 2f). Upon $Li_{1.13}Mn_{0.47}Ni_{0.2}Co_{0.2}O_2$ coating, the secondary particles exhibit inhomogeneous morphology and obvious agglomeration as a result of the partial fusion of primary particles.

Electrochemical characterization

Electrochemical properties of the samples were evaluated using a coin-type cell. Figure 3 a demonstrates the voltage profiles of the initial charge–discharge of lithium cells with the synthesized materials with a rate of 0.1 C between 2.0 and 4.8 V vs. Li^+/Li. The shape of the first charge–discharge curves of the coated sample is consistent with general Li-rich layered structure materials. During the first charge process, the cell voltages gradually increased up to 4.5–4.6 V and showed a long voltage plateau upon Li ion extraction. The plateau at 4.5 V is typical for the first charge process of Li-rich layered oxides. The irreversible lithium ion extracts and oxygen released from the monoclinic Li_2MnO_3-like domains correspond to the activation of the layered Li_2MnO_3-like region and the large irreversible capacity loss [33], resulting in the formation of the electrochemically active MnO_2 component [34].

The discharge-specific capacity of the samples increased upon coating with 3 wt% $Li_{1.13}Mn_{0.47}Ni_{0.2}Co_{0.2}O_2$. A lower irreversible capacity (77 mAh g^{-1}) resulted in higher initial coulombic efficiency. The first cycle efficiency slightly

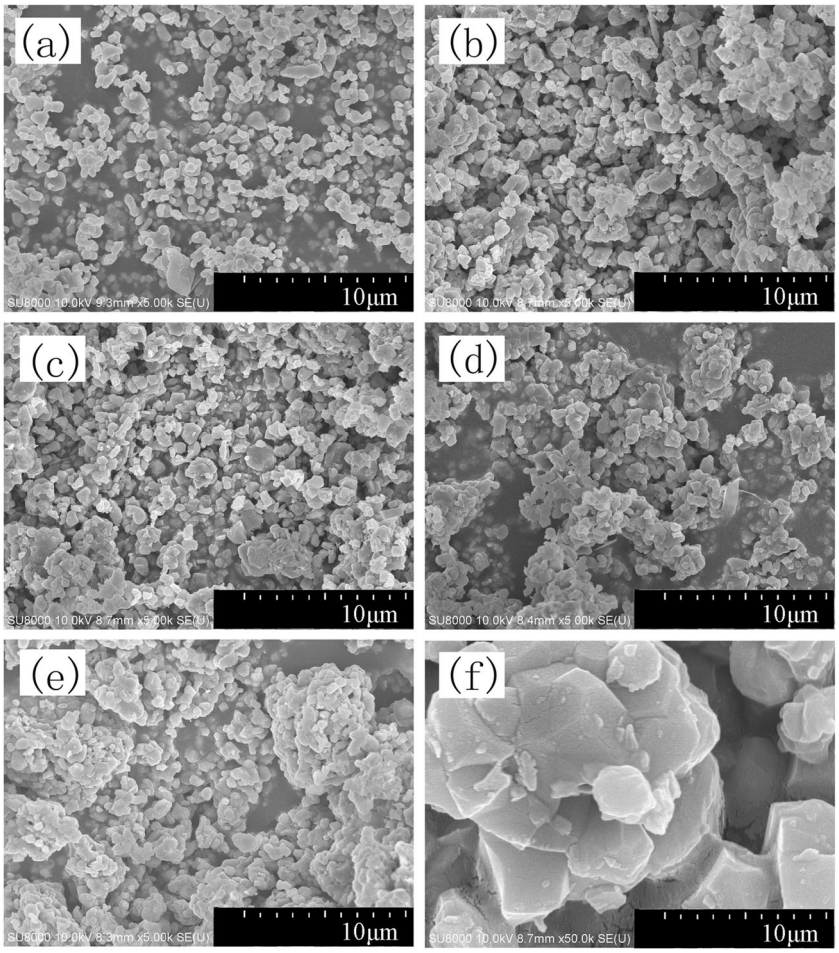

Fig. 2 SEM images of the as prepared samples. **a** M0. **b** M1. **c** M3. **d** M5. **e**, **f** M7

increased from 74.4% (sample M0) to 76.8% (sample M3). Li-rich layered oxides exhibited huge irreversibility owing to the permanent structural change during the first charge process. The oxygen release significantly decreased the efficiency of the material because the Li ions cannot be reintercalated into the host because of the lack of possible Li ion sites.

The coated samples showed significant reduction in the discharge-specific capacity with increasing coating quantity (> 3 wt%) in the first cycle. This result corresponds to the SEM results because larger particle sizes cause smaller reversible capacity due to increased Li ion diffusion length. As shown in Fig. 3a, the discharge profiles of 3 wt% coated sample are higher than those of the other samples. Hence, the appropriate content of $Li_{1.13}Mn_{0.47}Ni_{0.2}Co_{0.2}O_2$ can elevate the discharge potential plateau. The higher discharge potential plateau indicates the lower polarization of 3 wt% coated sample than the other materials.

The high initial charge–discharge performance of the coated sample could be mainly attributed to the presence of $Li_{1.13}Mn_{0.47}Ni_{0.2}Co_{0.2}O_2$. During the charge–discharge process for $Li[Li_{0.2}Mn_{0.52}Ni_{0.13}Co_{0.13}V_{0.02}]O_2$, $Li_{1.13}Mn_{0.47}Ni_{0.2}Co_{0.2}O_2$ participated in the electrochemical reaction and contributed to high charge–discharge specific capacity. The electronic conductivity and lithium ion diffusion of the coated materials were improved by the surface coating layers.

The reaction mechanism of the materials in charging and discharging was analyzed using the dQ/dV curves. Figures 3 b and c show the dQ/dV curves obtained using the discharge profiles in Fig. 3a. Two distinct oxidation peaks were observed in the first charging process. The oxidation peak at 3.9 to 4.0 V corresponds to the oxidation of Ni^{2+} into Ni^{4+} and Co^{3+} into Co^{4+} in the material. The oxidation peak at 4.45 V to 4.55 V corresponds to the loss of O^{2-} and Li^{+} in Li_2MnO_3. In the first discharge process, two distinct reduction peaks exist from 3.7 V to 3.8 V and from 3.4 V to 3.5 V. These peaks originate from the Li intercalation to delithiated $LiMeO_2$ and Li_2MnO_3 components. The addition of $Li_{1.13}Mn_{0.47}Ni_{0.2}Co_{0.2}O_2$ significantly increased the intensity of the peaks. These results indicate that the lower irreversibility of the coated materials could be due to the enhanced efficiency of Li re-insertion into the delithiated Li_2MnO_3 component. A small discharge peak was observed at 2.5 to 2.6 V. A small amount of spinel-like phase likely existed in the materials. Hence, the $Li_{1.13}Mn_{0.47}Ni_{0.2}Co_{0.2}O_2$ coating layer could not only effectively restrain the reaction between the

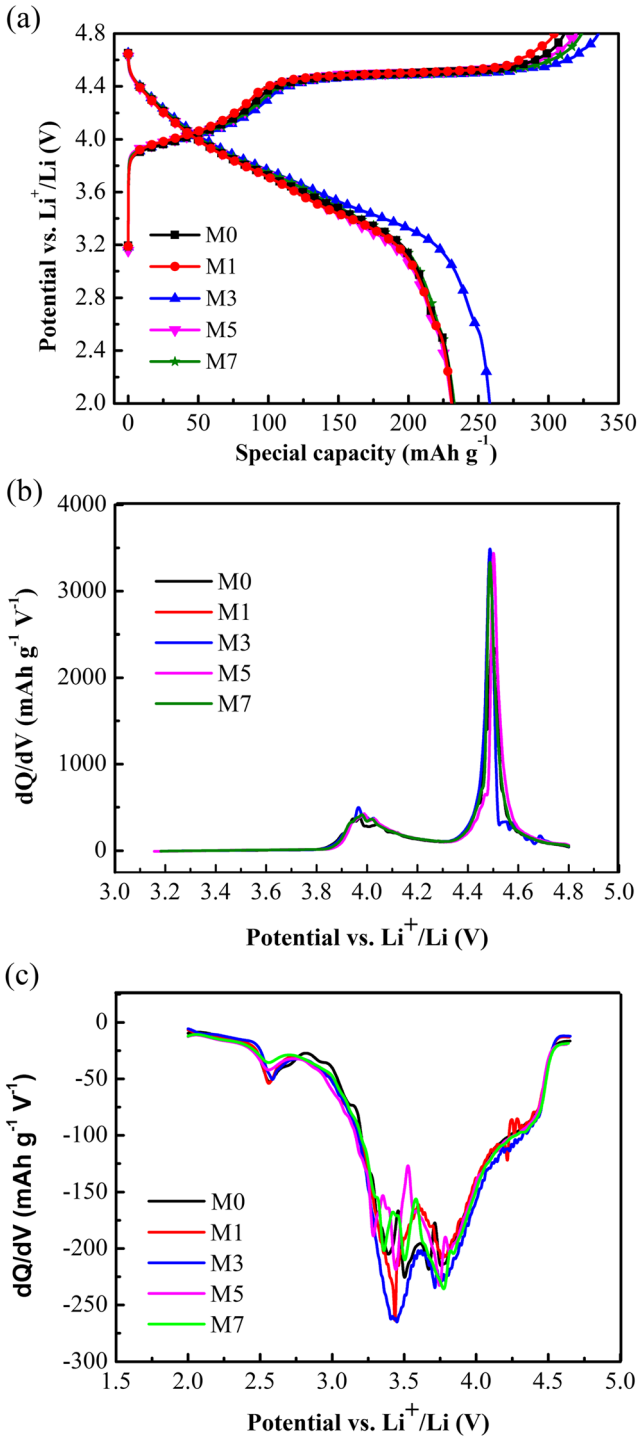

Fig.3 **a** Initial charge–discharge curves of samples. **b** dQ/dV curves of samples during the initial charging process. **c** dQ/dV curves of samples during the initial discharging process

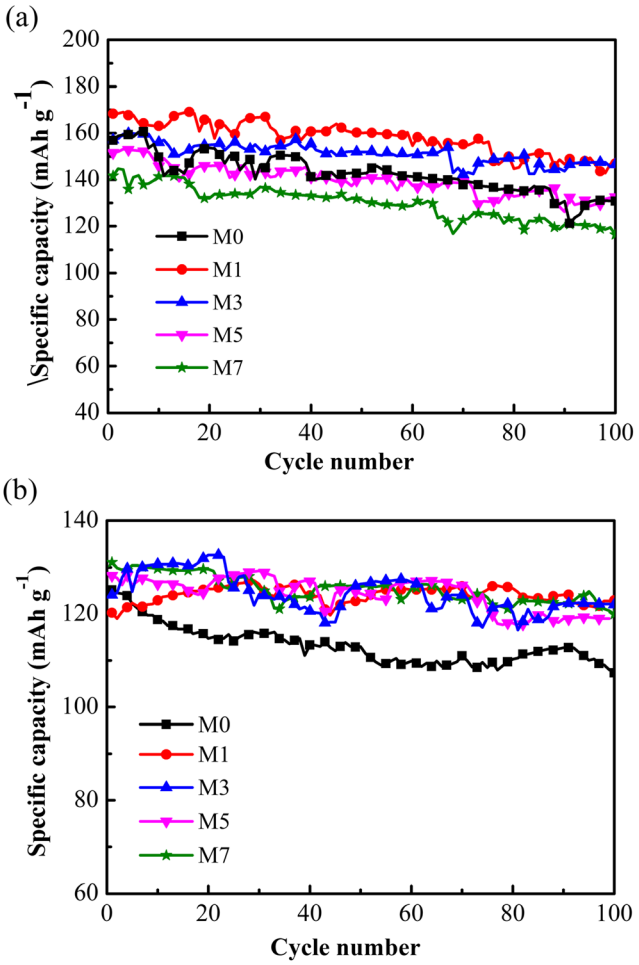

Fig. 4 Cycle performance of samples at **a** 1 C and **b** 5 C rate

$Li[Li_{0.2}Mn_{0.52}Ni_{0.13}Co_{0.13}V_{0.02}]O_2$ particles and the electrolyte but also promote the formation of SEI film with improved structure on the cathode surface.

Cycle performance of the lithium cells with the synthesized materials used as cathodes was recorded at rates of 1 C and 5 C within the voltage range of 2.0 to 4.8 V (Fig. 4). The coated samples exhibited sufficient advantages in cycles. Compared with the cyclic performance of these cathode materials, 1 to 3 wt% coated materials demonstrated the best cycling performance at 1 C. All coated materials exhibited better cycle performance than the uncoated sample at 5 C. After 100 cycles at 1 C, the normalized specific capacity retentions for the samples M0, M1, M3, M5, and M7 are 83.4%, 87.3%, 93.2%, 87.4%, and 82.2%, respectively. The specific capacity retention of 3 wt% coated material is 11.8% higher than that of the uncoated one. All the $Li_{1.13}Mn_{0.47}Ni_{0.2}Co_{0.2}O_2$-coated materials delivered higher discharge capacity and capacity retention compared with the blank sample at 5 C after 100 cycles. All the coated materials delivered a capacity of 120–130 mAh g^{-1} in the 100th cycle, which is larger than that of the blank sample (107 mAh g^{-1}). This finding implies that $Li_{1.13}Mn_{0.47}Ni_{0.2}Co_{0.2}O_2$-coating is an effective method for improving the discharge capacity and cycling performance of $Li[Li_{0.2}Mn_{0.52}Ni_{0.13}Co_{0.13}V_{0.02}]O_2$ materials at high discharge rates. The $Li_{1.13}Mn_{0.47}Ni_{0.2}Co_{0.2}O_2$ coating layer can hinder materials from directly contacting the electrolyte to protect them against erosion in the electrolyte, thereby stabilizing their structure. Therefore, the cycling stability of the

materials was significantly improved. The protection of the $Li_{1.13}Mn_{0.47}Ni_{0.2}Co_{0.2}O_2$ coating layer becomes more obvious with increasing discharge rate.

As one of the most important performance parameters, the rate capability of the coated materials is better than that of the uncoated Li-rich material at various discharge rates within the voltage range of 2.0–4.8 V (Fig. 5). The discharge capacity for all materials gradually decreased with increasing discharge rate due to the increased polarization at high current density. All the samples showed stable discharge-specific capacity at each rate for five times. The materials coated with $Li_{1.13}Mn_{0.47}Ni_{0.2}Co_{0.2}O_2$ delivered higher discharge capacity at different discharge rates than that of the uncoated one. These results indicate that the rate performance of Li-rich materials was improved by $Li_{1.13}Mn_{0.47}Ni_{0.2}Co_{0.2}O_2$ coating at various discharge rates. When the coating amount is 3 wt%, the material delivered the highest discharge-specific capacity at various rates. The specific capacity of sample M3 is 115.9 mAh g^{-1} at 5 C, and that of sample M0 is 89.8 mAh g^{-1} under the same condition. This finding implies that surface modification with $Li_{1.13}Mn_{0.47}Ni_{0.2}Co_{0.2}O_2$ can greatly improve the rate performance of the material. Therefore, the outstanding rate capacity for the coated $Li[Li_{0.2}Mn_{0.52}Ni_{0.13}Co_{0.13}V_{0.02}]O_2$ proves that $Li_{1.13}Mn_{0.47}Ni_{0.2}Co_{0.2}O_2$ coating layer could not only effectively restrain the reaction between the $Li[Li_{0.2}Mn_{0.52}Ni_{0.13}Co_{0.13}V_{0.02}]O_2$ particles and electrolyte but also promote Li^+ transport. The $Li_{1.13}Mn_{0.47}Ni_{0.2}Co_{0.2}O_2$ coating layer can accelerate Li^+ transport and improve ion exchange during the charge–discharge process.

Electrochemical impedance spectroscopy measurements were performed for blank sample and $Li_{1.13}Mn_{0.47}Ni_{0.2}Co_{0.2}O_2$-coated materials to evaluate the enhanced electrochemical properties and investigate the electrochemical kinetics of materials (Fig. 6). In general, the Nyquist plot of Li-rich materials consists of the following parts: the high-frequency semicircle is connected to the lithium ion migration through the solid electrolyte interface (SEI) membrane and coated layer; the medium-frequency semicircle reflects the charge-transfer process (Rct) at the electrode/electrolyte interface; and the low-frequency slope corresponds to the Warburg impedance that is correlated with lithium ion diffusion. All the samples exhibited small internal resistance of the cell, indicating their negligible ohmic polarization. The Rct decreased first and then increased with increasing coating quantity. Hence, applying a suitable coating layer can reduce the charge-transfer resistance of materials.

Cyclic voltammograms of samples were recorded to further evaluate the redox reaction and phase transformation during the charge–discharge process (Fig. 7). All the samples exhibited two anodic peaks at 4.1 V and 4.6 V in the first cycle, which are related to the two voltage plateaus in the initial charge curves. The anodic peak at 4.1 V corresponds to the lithium extraction from the $LiMO_2$ (M = Ni, Co, or Mn) phase and to the oxidation of Ni^{2+} to Ni^{4+} and Co^{3+} to Co^{4+}. Meanwhile, the anodic peak at 4.6 V is due to Li_2O elimination from Li_2MnO_3 to form MnO_2. For all the samples, the two cathodic peaks at 3.7 V and 4.4 V are attributed to the reduction of transition metal ions (Ni^{4+} to Ni^{2+} and Co^{4+} to Co^{3+}, respectively). In the second and third cycles, the cathodic peak at 3.3 V is due the reduction of Mn^{4+} into Mn^{3+}, which indicates the transformation from the layered structure to the spinel structure [35]. Compared with the uncoated material, $Li[Li_{0.2}Mn_{0.52}Ni_{0.13}Co_{0.13}V_{0.02}]O_2$ coated with $Li_{1.13}Mn_{0.47}Ni_{0.2}Co_{0.2}O_2$ shows a lower peak at 3.3 V. Hence, the coating layer can restrain the structural transformation for Li-rich layered oxides during cycling.

Conclusions

$Li_{1.13}Mn_{0.47}Ni_{0.2}Co_{0.2}O_2$-coated $Li[Li_{0.2}Mn_{0.52}Ni_{0.13}Co_{0.13}V_{0.02}]O_2$ materials were fabricated

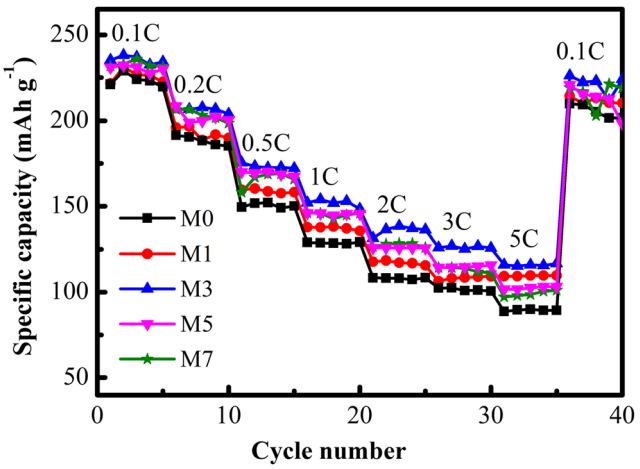

Fig. 5 Rate capability of samples between 2.0 and 4.8 V

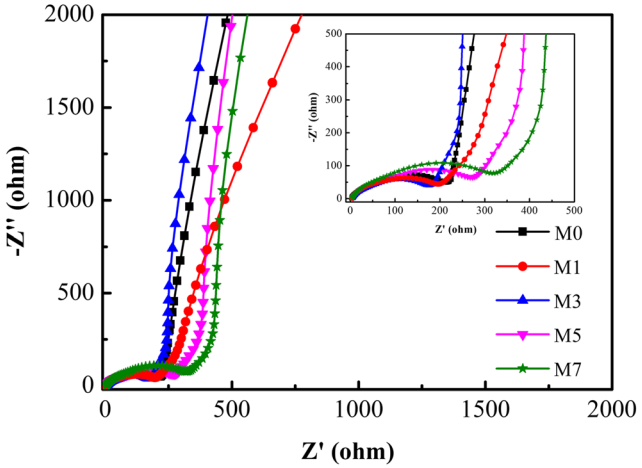

Fig. 6 Nyquist plots of samples

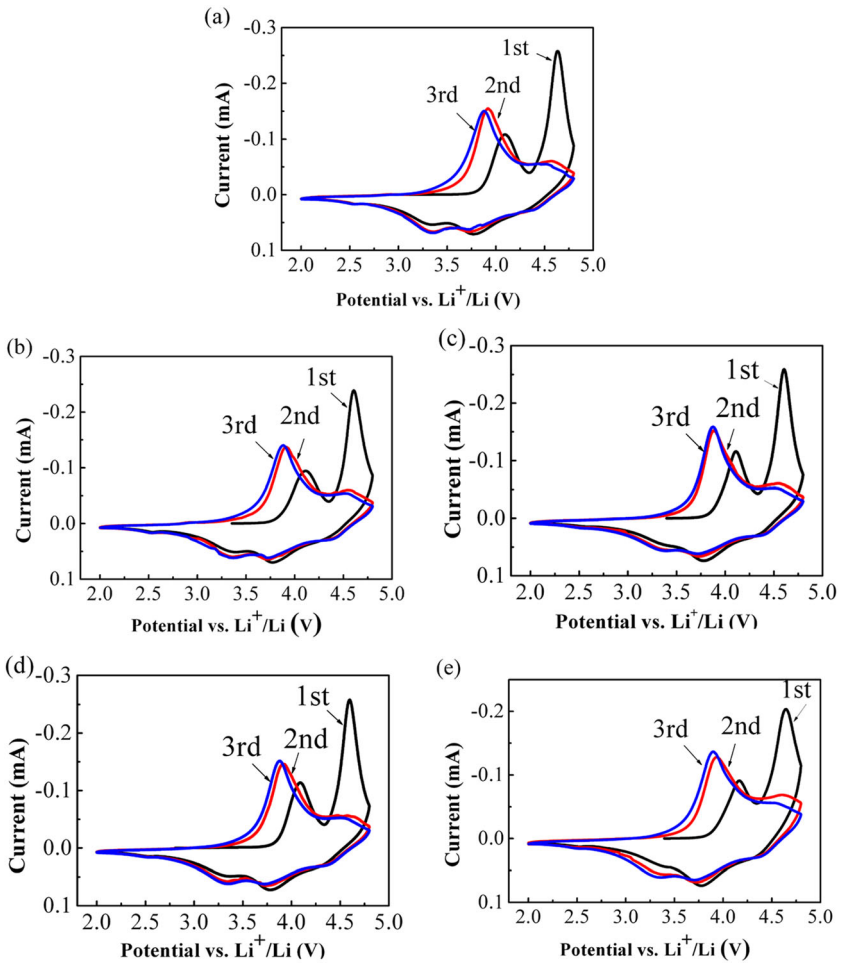

Fig. 7 Cycle voltammograms of samples **a** M0, **b** M1, **c** M3, **d** M5, and **e** M7 between 2.0 and 4.8 V at a scan rate of 0.1 mV s^{-1}

via a sol–gel method. $Li_{1.13}Mn_{0.47}Ni_{0.2}Co_{0.2}O_2$ particles were coated on $Li[Li_{0.2}Mn_{0.52}Ni_{0.13}Co_{0.13}V_{0.02}]O_2$ particles, and the $Li_{1.13}Mn_{0.47}Ni_{0.2}Co_{0.2}O_2$ coating had no obvious effect on the crystal structure of Li-rich materials. The cycle performance and rate capability of the Li-rich materials coated with $Li_{1.13}Mn_{0.47}Ni_{0.2}Co_{0.2}O_2$ were significantly improved. The 1 to 3 wt% coated materials exhibited the best cycling performance at 1 C, and all coated materials exhibited better cycling performance than the uncoated one at 5 C. The $Li_{1.13}Mn_{0.47}Ni_{0.2}Co_{0.2}O_2$-coated materials delivered a capacity of 120 to 130 mAh g^{-1} in the 100th cycle at 5 C, which is larger than that of the blank sample (107 mAh g^{-1}). When the coating amount was 3 wt%, the material delivered the highest discharge-specific capacity at various rates. The specific capacity of 3 wt% $Li_{1.13}Mn_{0.47}Ni_{0.2}Co_{0.2}O_2$-coated material was 115.9 mAh g^{-1} at 5 C, and that of the blank sample was 89.8 mAh g^{-1} under the same condition. The improved electrochemical performance of the $Li_{1.13}Mn_{0.47}Ni_{0.2}Co_{0.2}O_2$-coated material can be ascribed to the $Li_{1.13}Mn_{0.47}Ni_{0.2}Co_{0.2}O_2$ layer that reduced the side reactions between the cathodes and electrolyte, restrained the structural transformation with cycling, and reduced the charge-transfer resistance. Therefore, $Li_{1.13}Mn_{0.47}Ni_{0.2}Co_{0.2}O_2$ coating could effectively enhance the electrochemical properties of Li-rich layered oxides.

Funding information This work was financially supported by the National Key Laboratory Foundation of China (Grant No. 6142808020117C01).

References

1. Goodenough JB, Kim Y (2010) Challenges for rechargeable Li batteries. Chem Mater 22:587–603
2. Zuo XX, Fan CJ, Xiao X, Liu JS, Nan JM (2012) High-voltage performance of $LiCoO_2$/graphite batteries with methylene methanedisulfonate as electrolyte additive. J Power Sources 219: 94–99
3. Min K, Seo SW, Song YY, Lee HS, Cho E (2017) A first-principles study of the preventive effects of Al and Mg doping on the degradation in $LiNi_{0.8}Co_{0.1}Mn_{0.1}O_2$ cathode materials. Phys Chem Chem Phys 3:1762–1769
4. Hu M, Pang XL, Zhou Z (2013) Recent progress in high-voltage lithium ion batteries. J Power Sources 237:229–242
5. Xi YK, Liu Y, Zhang DK, Jin SL, Zhang R, Jin ML (2018) Comparative study of the electrochemical performance of

$LiNi_{0.5}C_{o0.2}Mn_{0.3}O_2$ and $LiNi_{0.8}Co_{0.1}Mn_{0.1}O_2$ cathode materials for lithium ion batteries. Solid State Ionics 327:27–31
6. Huang MX, Sun YH, Guan DC, Nan JM, Cai YP (2019) Hydrothermal synthesis of mesoporous SnO_2 as a stabilized anode material of lithium-ion batteries. Ionics 25(12):5745–5757
7. Bian M, Yang Y, Tian L (2018) Carbon-free $Li_4Ti_5O_{12}$ porous nanofibers as high-rate and ultralong-life anode materials for lithium-ion batteries. J Phys Chem Solids 113:11–16
8. Zhang HZ, Zhang YT, Song DW, Shi XX, Zhang LQ, Bie LJ (2017) Tailoring the $(Ni_{1/6}Co_{1/6}Mn_{4/6})CO_3$ precursors of Li-rich layered oxides for advanced lithium-ion batteries with the seed-mediated method. J Alloys Compd 709:692–699
9. Sun G, Jia CX, Zhang JN, Hou LY, Ma ZP, Shao GJ, Wang ZB (2019) Core-shell structure $LiNi_{1/3}Mn_{1/3}Co_{1/3}O_2$@ ultrathin delta-$MnO_2$ nanoflakes cathode material with high electrochemical performance for lithium-ion batteries. Ionics 25(11):5249–5258
10. Manthiram A, Knight JC, Myung ST, Oh SM, Sun YK (2016) Nickel-rich and lithium-rich layered oxide cathodes: progress and perspectives. Adv Energy Mater 6:1501010–1501032
11. Zhang LS, Zhao ZJ, Cao Y, Wang LZ, Fang H, Gao KZ, Zhang AQ, Gao HL, Song YH (2019) In situ synthesis of porous $LiNi_{0.5}Co_{0.2}Mn_{0.3}O_2$ tubular-fiber as high-performance cathode materials for Li-ion batteries. Ionics 25(11):5229–5237
12. Zhao TL, Gao XY, Wei ZJ, Guo KJ, Wu F, Li L, Chen RJ (2018) Three-dimensional $Li_{1.2}Ni_{0.2}Mn_{0.6}O_2$ cathode materials synthesized by a novel hydrothermal method for lithium-ion batteries. J Alloys Compd 757:16–23
13. Xu CS, Yu HT, Guo CF, Xie Y, Ren N, Yi TF, Zhang GX (2019) Surface modification of $Li_{1.2}Mn_{0.54}Ni_{0.13}Co_{0.13}O_2$ via an ionic conductive LiV_3O_8 as a cathode material for Li-ion batteries. Ionics 25(10):4567–4576
14. Wang LZ, Yang W, Lv TF, Gao KZ, Yan J (2019) Adorned Li-rich $Li_{1.2}Ni_{0.13}Co_{0.13}Mn_{0.54}O_2$ with $LiAlO_2$ for improved electrochemical properties in lithium-ion batteries. Ionics 25(12):5681–5688
15. Ma J, Li B, An L, Wei H, Wang XY, Yu PR, Xia DG (2015) A highly homogeneous nanocoating strategy for Li-rich Mn-based layered oxides based on chemical conversion. J Power Sources 277:393–402
16. Chong SK, Chen YZ, Yan WW, Guo SW, Tan Q, Wu YF, Jiang T, Liu YN (2016) Suppressing capacity fading and voltage decay of Li-rich layered cathode material by a surface nano-protective layer of CoF_2 for lithium-ion batteries. J Power Sources 332:230–239
17. Song JH, Shim JH, Kapylou A, Yeon DH, Lee DH, Kim DH, Park JH, Kang SH (2016) Suppression of voltage depression in Li-rich layered oxide by introducing GaO_4 structural units in the Li_2MnO_3-like nano-domain. Nano Energy 30:717–727
18. Li JG, Li JL, Yu TH, Ding FX, Xu GF, Li ZY, Zhao YG, Kang FY (2016) Stabilizing the structure and suppressing the voltage decay of $Li[Li_{0.2}Mn_{0.54}Co_{0.13}Ni_{0.13}]O_2$ cathode materials for Li-ion batteries via multifunctional proxide surface modification. Ceram Int 42:18620–18630
19. Xie YX, Chen SZ, Yang W, Zou HB, Lin ZY, Zhou JC (2018) Improving the rate capability and decelerating the voltage decay of Li-rich layered oxide cathodes by constructing a surface-modified microrod structure. J Alloys Compd 772:230–239
20. Su N, Lyu YC, Gu R, Guo BK (2018) Al_2O_3 coated $Li_{1.2}Ni_{0.2}Mn_{0.2}Ru_{0.4}O_2$ as cathode material for Li-ion batteries. J Alloys Compd 741:398–403
21. Rastgoo-Deylami M, Javanbakht M, Omidvar H (2019) Enhanced performance of layered $Li_{1.2}Mn_{0.54}Ni_{0.13}Co_{0.13}O_2$ cathode material in Li-ion batteries using nanoscale surface coating with fluorine-doped anatase TiO_2. Solid State Ionics 331:74–88
22. Zheng FH, Ou X, Pan QC, Xiong XH, Yang CH, Liu ML (2017) The effect of composite organic acid (citric acid & tartaric acid) on microstructure and electrochemical properties of $Li_{1.2}Mn_{0.54}Ni_{0.13}Co_{0.13}O_2$ Li-rich layered oxides. J Power Sources 346:31–39
23. Jo CH, Cho DH, Noh HJ, Yashiro H, Sun YK, Myung ST (2015) An effective method to reduce residual lithium compounds on Ni-rich $Li[Ni_{0.6}Co_{0.2}Mn_{0.2}]O_2$ active material using a phosphoric acid derived Li_3PO_4 nanolayer. Nano Res 8:1464–1479
24. Yuan B, Liao SX, Xin Y, Zhong YJ, Shi XX, Li LY, Guo XD (2015) Cobalt-doped lithium-rich cathode with superior electrochemical performance for lithium-ion batteries. RSC Adv 5:2947–2951
25. Wang YX, Shang KH, He W, Ai XP, Cao YL, Yang HX (2015) Magnesium-doped $Li_{1.2}[Co_{0.13}Ni_{0.13}Mn_{0.54}]O_2$ for lithium-ion battery cathode with enhanced cycling stability and rate capability. ACS Appl Mater Interfaces 7:13014–13021
26. Yu RZ, Wang XY, Fu YQ, Wang LW, Cai SY, Liu MH, Lu B, Wang G, Wang D, Ren QF, Yang XK (2016) Effect of magnesium doping on properties of lithium-rich layered oxide cathodes based on a one-step co-precipitation strategy. J Mater Chem A 4:4941–4951
27. Guo B, Zhao JH, Fan XM, Zhang W, Li S, Yang ZH, Chen ZX, Zhang WX (2017) Aluminum and fluorine Co-doping for promotion of stability and safety of lithium-rich layered cathode material. Electrochim Acta 236:171–179
28. Zhao TL, Li L, Chen RJ, Wu HM, Zhang XX, Chen S, Xie M, Wu F, Lu J, Amine K (2015) Design of surface protective layer of LiF/FeF_3 nanoparticles in Li-rich cathode for high-capacity Li-ion batteries. Nano Energy 15:164–176
29. Li CD, Xu J, Xia JS, Liu W, Xiong X, Zheng ZA (2016) Influences of FeF_3 coating layer on the electrochemical properties of $Li[Li_{0.2}Mn_{0.54}Ni_{0.13}Co_{0.13}]O_2$ cathode materials for lithium-ion batteries. Solid State Ionics 292:75–82
30. Shi SJ, Tu JP, Mai YJ, Zhang YQ, Tang YY, Wang XL (2012) Structure and electrochemical performance of CaF_2 coated $LiMn_{1/3}Ni_{1/3}Co_{1/3}O_2$ cathode material for Li-ion batteries. Electrochim Acta 83:105–112
31. Cho SW, Kim GO, Ryu KS (2012) Sulfur anion doping and surface modification with $LiNiPO_4$ of a $Li[Co_{0.1}Ni_{0.15}Li_{0.2}Mn_{0.55}]O_2$ cathode material for Li-ion batteries. Solid State Ionics 206:84–90
32. Yuan W, Zhang HZ, Liu Q, Li GR, Gao XP (2014) Surface modification of $Li(Li_{0.17}Ni_{0.2}Co_{0.05}Mn_{0.58})O_2$ with CeO_2 as cathode material for Li-ion batteries. Electrochim Acta 135:199–207
33. Lu C, Wu H, Zhang Y, Liu H, Chen BJ, Wu NT, Wang S (2014) Cerium fluoride coated layered oxide $Li_{1.2}Mn_{0.54}Ni_{0.13}Co_{0.13}O_2$ as cathode materials with improved electrochemical performance for lithium ion batteries. J Power Sources 267:682–691
34. Thackeray MM, Johnson CS, Vaughey JT, Li N, Hackney SA (2005) Advances in manganese-oxide 'composite' electrodes for lithium-ion batteries. J Mater Chem 15:2257–2267
35. Sun YK, Lee MJ, Yoon CS, Hassoun J, Amine K, Scrosati B (2012) The role of AlF_3 coatings in improving electrochemical cycling of Li-enriched nickel-manganese oxide electrodes for Li-ion batteries. Adv Mater 24:1192–1196